Rapid Communications

Spectra of heavy polarons and molecules coupled to a Fermi sea

Dimitri Pimenov[1,*] and Moshe Goldstein[2]

[1]*Arnold Sommerfeld Center for Theoretical Physics, Ludwig-Maximilians-University Munich, 80333 Munich, Germany*

[2]*Raymond and Beverly Sackler School of Physics and Astronomy, Tel Aviv University, Tel Aviv 6997801, Israel*

(Received 18 September 2018; published 12 December 2018)

We study the spectrum of an impurity coupled to a Fermi sea (e.g., minority atom in an ultracold gas, exciton in a solid) by attraction strong enough to form a molecule/trion. We introduce a diagrammatic scheme which allows treating a finite mass impurity while reproducing the Fermi-edge singularity in the immobile limit. For large binding energies the spectrum is characterized by a semicoherent repulsive polaron and an incoherent molecule-hole continuum, which is the lowest-energy feature in the single-particle spectrum. The previously predicted attractive polaron seems not to exist for strong binding.

DOI: 10.1103/PhysRevB.98.220302

Introduction. The interaction of a single impurity with a surrounding fermionic bath is a problem at the very heart of quantum many-body physics, which is easily formulated, and yet difficult to solve. It is characterized by a rich interplay of kinetic and interaction effects, which can strongly modify the quasiparticle (polaronic) nature of the impurity. Controlled experimental realization and analysis of impurity physics has recently been achieved in ultracold gas setups [1–5], where the impurity is usually an excited hyperfine state of an atom, and the interaction strength is tunable via Feshbach resonances [6]. An alternative are semiconductor or transition metal dichalcogenide (TMD) experiments [7,8], where the impurity is a valence band hole or exciton, in the presence of a finite conduction band population controlled by gate voltage.

On the theory side, a major part of the literature is devoted to the computation of ground-state energies following Chevy's [9] pioneering work, which proposed an ansatz for the ground-state wave function consisting of the impurity dressed by a single electron-hole pair. This ansatz works well in the polaronic regime where the impurity-bath interaction is weak, but breaks down if the formation of a molecule, or trion in semiconductor language, becomes favorable. This regime can be described by a complementary ansatz [10–12] involving a dressed molecule. In two dimensions (2D), a similar picture applies [13–15].

The variational energy has recently been verified using diagrammatic quantum Monte Carlo [16–21]. The situation is quite different for the *impurity spectrum*, which is the actual quantity measured in experiments: In Monte Carlo, extracting the spectrum is difficult due to the infamous analytical continuation problem, and only few definite statements can be made [22]. Analytically, it has been realized that the Chevy ansatz is equivalent to the non-self-consistent T-matrix approach [23], from which spectra can be easily extracted [1,5,8,24–26]. However, this ansatz is *a priori* reliable for weak coupling only. In the molecule limit, extracting the spectrum from a variational ansatz is difficult since the coefficients are not analytically known. As for the functional renormalization group [27], its accuracy is hard to assess [28].

Besides the interaction strength and Fermi energy, a third control parameter in the impurity problem is the impurity mass M. Infinitely heavy impurities are subject to Anderson orthogonality [29], and the universal properties of the impurity spectrum in the presence of a bound state can be computed exactly from a functional determinant [30–33]. The goal of this Rapid Communication is to characterize the spectrum for arbitrary impurity mass, while maintaining consistency with all known limits. Building on the framework developed in our recent work [34], we find that a rigorous expansion in the number of fermion-hole pairs reproduces the infinite mass spectrum, and obtain controlled estimates of the impurity spectrum deep in the molecular limit; in particular, we present a controlled computation of the incoherent molecular feature in the single-particle spectrum. We mostly focus on 2D for clarity, listing the modifications in 3D along the way.

Model. Consider a single impurity (annihilation operator d) immersed in a bath of fermions (c). In a cold atom system, the impurity can be a spin-up fermion in a bath of spin-down particles; in semiconducting systems, the impurity is usually an exciton containing a conduction electron with a given spin, together with a bath of the opposite spin conduction electrons [35]. The usual model Hamiltonian reads

$$H = \sum_{\mathbf{k}} (\epsilon_{\mathbf{k}} c_{\mathbf{k}}^\dagger c_{\mathbf{k}} + E_{\mathbf{k}} d_{\mathbf{k}}^\dagger d_{\mathbf{k}}) - \frac{V_0}{\mathcal{S}} \sum_{\mathbf{k},\mathbf{p},\mathbf{q}} c_{\mathbf{k}}^\dagger c_{\mathbf{k}-\mathbf{q}} d_{\mathbf{p}}^\dagger d_{\mathbf{p}+\mathbf{q}}, \quad (1)$$

with $\epsilon_{\mathbf{k}} = k^2/2m$, $E_{\mathbf{k}} = k^2/2M$. $V_0 > 0$ is the attractive contact interaction [36], $\mathcal{S}$ the system area, and $\hbar = 1$. Our goal is to find the single-particle spectrum $\mathcal{A}(\omega)$ at zero momentum, which is proportional to the Fourier transform of the imaginary part of the retarded impurity Green's function, $D(t) = -i\theta(t)\,\langle 0|d_0(t)d_0^\dagger(0)|0\rangle$, where $|0\rangle$ is the Fermi sea without impurity. We work in the real frequency formalism at zero temperature.

Chevy's ansatz versus the Fermi-edge singularity. Chevy's ansatz corresponds to a summation of all impurity self-energy diagrams Σ_1 with a single hole (the T-matrix series), shown

*D.Pimenov@physik.lmu.de

 ©2018 American Physical Society

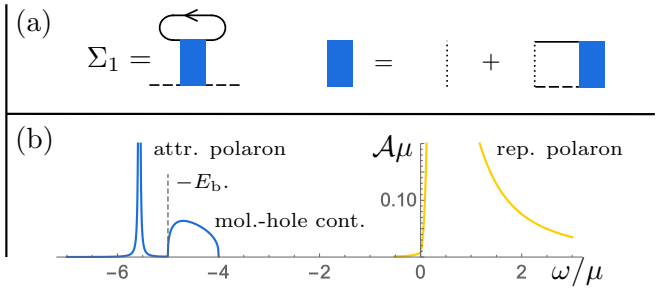

FIG. 1. (a) Self-energy diagrams with one hole, indicated by the arrow. Solid (dashed) lines denote electron (impurity) propagators. The blue box indicates the T matrix. (b) ($M = \infty$) spectrum for $E_b = 5\mu$ from the Chevy ansatz. Repulsive and attractive features in the spectrum are shown in different colors for clarity. For the attractive polaron, a finite width is used.

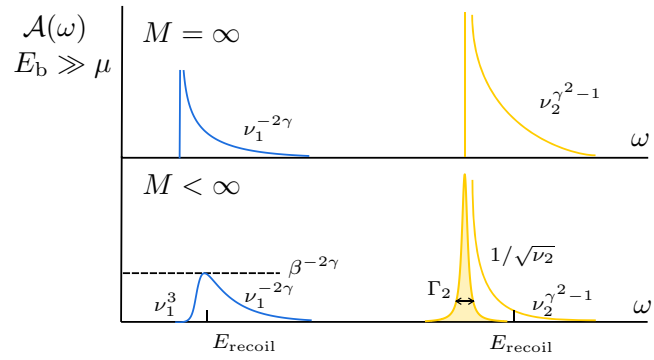

FIG. 2. Sketch of the spectrum for $E_b \gg \mu$. Power laws are measured from the respective thresholds; $\Gamma_2 \simeq \mu^4/E_b{}^4\beta$ is the width of the repulsive polaron (see main text). Colors are chosen as in Fig. 1.

in Fig. 1(a). For infinite mass, one finds, in 2D,

$$\Sigma_1(\omega) = -\int_0^\mu d\epsilon_{\mathbf{k}} \frac{1}{\ln\left(\frac{\omega+\epsilon_{\mathbf{k}}-\mu+i0^+}{-E_b}\right)}. \tag{2}$$

Here, ω is the energy measured from the impurity level, and $\mu = k_F^2/2m$ is the Fermi energy. We define the complex logarithm with a branch cut on the negative half axis. $-E_b$ is the energy of the bound state of the attractive contact potential, which always exists in 2D. It is determined from the pole of the T matrix. Due to this bound state, $\mathrm{Im}[\Sigma_1](\omega)$ has a molecule continuum $\propto\theta(\omega + E_b)$. Its width is μ, representing the different energies of the hole in the Fermi sea created when the impurity binds an electron. For $E_b \gg \mu$, inserting Σ_1 into the bare impurity Green's function $D_0(\omega) = 1/(\omega + i0^+)$ leads to three prominent features: First, the bare pole of the impurity is shifted ("repulsive polaron"). Second, the aforementioned molecule-hole continuum is created. Third, $\mathrm{Re}[\Sigma_1]$ gives rise to another pole below the molecule-hole continuum, the "attractive polaron." Between the latter two there is a spectral gap of $\simeq -0.582\mu$ as $E_b/\mu \to \infty$ [13]. A typical plot is shown in Fig. 1(b). The 3D result is similar (see Supplemental Material [37]). For finite mass, expression (2) is more complicated, but the qualitative form of the spectrum is unchanged [25].

The "Chevy" spectrum for $M = \infty$ is to be contrasted with the exact result of Combescot and Nozières [30], who showed that the spectrum is dominated by two divergent power laws [38] $\mathcal{A}(\omega) \propto \sum_{i=1,2}(\omega - \omega_{\mathrm{th},i})^{\alpha_i}\theta(\omega - \omega_{\mathrm{th},i})$. Here, $\omega_{\mathrm{th},i}$ are the threshold energies determined from Fumi's theorem [39], and the exponents α_i are characterized by δ, the phase shift of the bath fermions at the Fermi energy due to their scattering by the immobile impurity, $\alpha_1 = (\delta/\pi)^2 - 1$, $\alpha_2 = (1 - \delta/\pi)^2 - 1$. For infinite mass, the dimensionality of the problem only affects the value of δ. For $E_b \gg \mu$ one can then approximate [40,41]

$$1 \gg 1 - \delta/\pi \simeq \gamma \equiv \begin{cases} 1/\ln(E_b/\mu) & \text{for } d = 2, \\ k_F a/\pi & \text{for } d = 3, \end{cases} \tag{3}$$

with the 3D scattering length a. In this limit, with exponents to leading order in γ, the spectrum looks like

$$\mathcal{A}(\omega) \simeq \theta(\nu_1)\nu_1^{-2\gamma} + \theta(\nu_2)\nu_2^{\gamma^2-1}, \quad \nu_i \equiv \omega - \omega_{\mathrm{th},i}. \tag{4}$$

A sketch is shown in Fig. 2 (upper panel). The lower (blue) feature, which starts close to $\omega = -E_b$ and corresponds to the molecule-hole continuum, has a weak power law (close to a step). The upper feature, which can be identified with the repulsive polaron, has a strong power-law spectrum (close to a delta function). Note that there is no well-defined "attractive polaron" in the spectrum. We claim that, for $E_b \gg \mu$, this will persist for finite masses M, and thus the Chevy spectrum of Fig. 1(b) is incorrect *for large binding energies*.

Method. Our approach is to reproduce Eq. (4) in a diagrammatic expansion in γ generalizable to finite mass. However, γ does not directly appear in the Hamiltonian; instead, one must resort to an expansion in the *number of holes*: A diagram involving n holes contains n integrations over filled states $\propto\mu^n$, and μ is small in units of E_b. In effect, as shown below, this leads to an expansion in γ [12,14,15,23,42].

The one-hole diagrams are already considered as the impurity self-energy within the Chevy approach [Fig. 1(a)], and resummed with Dyson's equation. For heavy impurities, this resummation is uncontrolled. Instead, one must add up the most important (log-divergent) diagrams order by order in γ, which ultimately removes the attractive polaron from the spectrum. Thus, we reattach the impurity lines to Σ_1, defining $H_1(\omega) = D_0(\omega)^2\Sigma_1(\omega)$. Of course, H_1 only represents the first-order process: The impurity can interact with an arbitrary number of electrons, creating electron-hole excitations in the Fermi sea. The processes involving two holes are represented in Fig. 3(a). Here, the interaction lines can be drawn arbitrarily often in any order, as long as the structure of the diagrams is preserved, e.g., in diagram H_2^a the first and last interaction lines should connect to the lower part of the "horseshoe," and to the upper loop in diagram H_2^c. These diagrams can also be redrawn with T-matrix blocks, as exemplarily shown in Fig. 3(b); we never expand in the number of T matrices, but always resum diagrams with an infinite number of T matrices at the two-hole level. We note that the contribution of the two-hole diagrams to the ground-state energy is much less significant [12,43].

Results: The molecule/attractive polaron spectrum. For dispersionless infinite mass impurities, the evaluation of all two-hole diagrams is possible. Following Ref. [34], one can either work in the time or frequency domain, employing

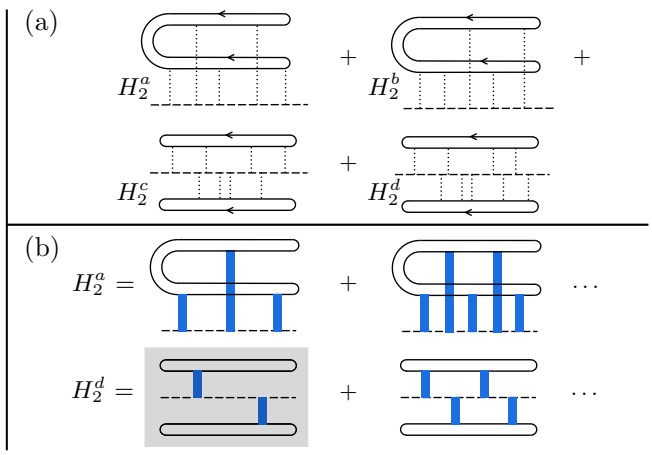

FIG. 3. (a) All relevant two-hole diagrams. (b) T-matrix representation of diagram series H_2^a, H_2^d. The gray-shaded diagram is contained in the Chevy approach.

different approximations [37]. In particular, for small $\omega + E_B$, close to the molecular threshold, we find [44]

$$H_1(\omega) + H_2(\omega) \simeq \frac{1}{E_\mathrm{b}}\left[\ln\left(\frac{\omega + E_\mathrm{b} + i0^+}{-\mu}\right) - \gamma \ln^2\left(\frac{\omega + E_\mathrm{b} + i0^+}{-\mu}\right)\right], \tag{5}$$

where $H_2 = \sum_i H_2^i$. The term $\propto \ln^2$ in Eq. (5) arises solely from diagram H_2^a. Curiously, the contribution of H_2^d is subleading, while the contribution from diagrams H_2^b, H_2^c effectively shifts the bound-state energy as $E_\mathrm{b} \to E_\mathrm{b} + \mu(1-\gamma)$ in 2D, or $E_\mathrm{b} + \mu(1 - 2\gamma/3)$ in 3D, in agreement with Fumi's theorem [39] to leading order in γ. Redefining ν_1 to include these shifts, we find a contribution to the spectrum,

$$\mathcal{A}_1(\nu_1) \simeq \frac{\theta(\nu_1)}{E_\mathrm{b}}(1 - 2\gamma \ln[\nu_1/\mu]), \tag{6}$$

in agreement with Eq. (4) when expanded in γ. This expansion has the same form as the perturbative expansion of the polarization in the standard Fermi-edge singularity case [45–47]. This was to be expected, as in the limit $E_\mathrm{b} \to \infty$ we can formally regard the diagrams $H_{1,2}$ as polarization diagrams containing a molecule and a bath fermion, with an effective molecule-bath interaction γ. We expect higher-order leading logarithmic (parquet) contributions to arise in a similar fashion from diagrams containing a larger number of holes.

Let us now address the modification of the molecule-hole feature for a large but finite impurity mass M. The general strategy is to reevaluate the frequency-domain diagrams of Fig. 3(b) for finite mass [37], and trace the modification of the logarithmic singularities [34,48–52]. Our results hold to leading order in the mass ratio $\beta = m/M$ only, but we expect them to be qualitatively correct all the way up to $\beta \simeq 1$. First, introducing a finite mass shifts the binding energy, $E_\mathrm{b} \to \tilde{E}_\mathrm{b}$, but we will not compute those shifts in detail, limiting ourselves to the form of the spectrum. In terms of $\nu_1 = \omega + \tilde{E}_\mathrm{b}$, the real part of the logarithmic singularities is modified as $\ln(\max[\nu_1 - \beta\mu, \gamma^2\beta\mu]/\mu)$, again reminiscent of the Fermi-edge singularity case [48]. In contrast to $M = \infty$, the logarithmic singularities for finite mass are peaked at $\nu_1 = \beta\mu$ ("direct threshold" [48]). This is simply understood: When an incoming zero momentum impurity binds an electron and leaves behind a low-energy hole, the resulting molecule must have a momentum $\simeq k_F$ by momentum conservation. Since the molecule is now mobile, with mass $M_+ = M + m$, one must pay its recoil energy $E_\mathrm{recoil} \simeq \beta\mu$, which shifts the maximum of the logarithms to $\nu_1 = \beta\mu$. Subsequently, the so created molecule can decay into a zero momentum state, by exciting an electron-hole pair. The rate of this indirect process is $\Gamma_1 = \gamma^2\beta\mu$, leading to a cutoff of the logarithmic singularities. Mathematically, this cutoff arises from the diagram H_2^c, which can be interpreted as a molecule self-energy diagram with an imaginary part Γ_1. For large frequencies, $\nu_1 \gg E_\mathrm{recoil}$, one recovers the infinite mass behavior $\propto \nu_1^{-2\gamma}$.

Apart from cutting off the singularity, the decay of the molecule leads to a shift of the threshold from the direct to the "indirect" one at $\nu_1 = 0$, which corresponds to the creation of zero momentum molecules. Near the indirect threshold, the spectrum starts continuously, with a power law $\propto \nu_1^3$ in 2D and $\propto \nu_1^{7/2}$ in 3D. This behavior is obtained by computing the imaginary parts of diagrams $H_2^{a,c}$, which yield the leading contributions in γ via standard phase space estimation [34,37]. For a spinless Fermi sea, the two contributions cancel; however, even in this case we expect that the power-law behavior is robust, since it is (a) determined from a generic phase space estimate and (b) there may well be processes involving three holes that yield the same behavior. Exponentiating the logarithms [34], one finds the spectrum near both thresholds to be

$$\mathcal{A}_1(\nu_1) \simeq \frac{1}{E_\mathrm{b}}\left(\frac{\sqrt{(\nu_1 - \beta\mu)^2 + (\gamma^2\beta\mu)^2}}{\mu}\right)^{-2\gamma} \theta(\nu_1) f_1(\nu_1), \tag{7}$$

where $f_1(\nu_1)$ smoothly interpolates between $f_1(\nu_1) \simeq \gamma^2(\nu_1/\beta\mu)^3$ in 2D and $f_1(\nu_1) \simeq \gamma^2(\nu_1/\beta\mu)^{7/2}$ in 3D, for $\nu_1 \ll \beta\mu$, and $f_1(\nu_1) \simeq \pi$ for $\nu_1 \gtrsim \beta\mu$. A typical plot of the resulting spectrum is shown in Fig. 2 (blue feature in the lower panel). Let us reiterate: The ground-state signal in the spectrum is purely incoherent, with maximum $\propto(\beta)^{-2\gamma}$ [53]; there is no polaronic delta peak.

Results: The repulsive polaron spectrum. We now discuss the repulsive polaron already predicted by the Chevy ansatz [5,14,27,54–56]. For $E_\mathrm{b} \gg \mu$, the repulsive polaron contains most of the spectral weight, $\sim 1 - \mu/E_\mathrm{b}$, as seen in Fig. 1(b): As $E_\mathrm{b}/\mu \to \infty$, the repulsive polaron is essentially a spectral probe of the impurity without the Fermi sea, with unit weight. For infinite mass, the asymptotic form of the repulsive polaron is given by the second term in Eq. (4), with $\omega_{\mathrm{th},2} \simeq \gamma\mu$ in 2D and $\omega_{\mathrm{th},2} \simeq \frac{2}{3}\gamma\mu$ in 3D. To leading order in γ, $\mathcal{A}_2(\nu_2) \simeq \gamma^2\theta(\nu_2)/\nu_2$, which reduces to a delta function as $\gamma \to 0$. This leading-order term can already be obtained from the first-order diagram H_1 for small positive frequencies. One can also reproduce the full power-law singularity in a linked cluster approach, formally exponentiating H_1. Extending the latter approach to finite mass, one finds a delta peak with weight β^{γ^2}, on top of an incoherent background $\propto 1/\sqrt{\nu_2}$

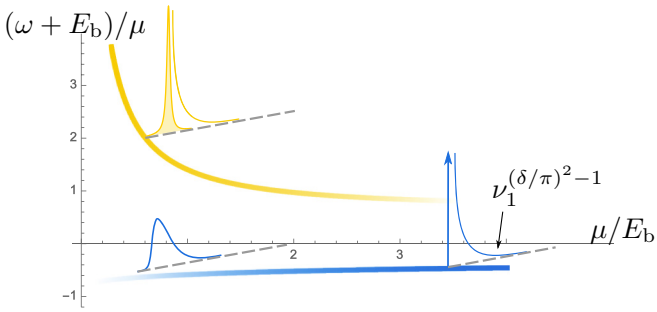

FIG. 4. Sketch of the full 2D spectrum for general values of μ/E_b. Thick lines indicate the threshold position determined from Fumi's theorem.

for $\nu_2 \ll \beta\mu$, similar to the results of Ref. [51]. In 3D, the incoherent part is approximately constant. For much larger frequencies $\nu_2 \gtrsim \beta\mu$, one recovers the infinite mass behavior $\propto \nu_2^{\gamma^2-1}$ [37].

Thus, in a first approximation, the repulsive polaron is a delta peak plus incoherent background. However, for finite mass, the delta peak may be broadened due to decay into the low-lying molecule-hole continuum, resulting in a finite width Γ_2. This width can be estimated by computing the self-energy part of the diagrams H_2 (called Σ_2) at the repulsive polaron threshold $\nu_2 = 0$. Note that, for infinite mass, the problem becomes single particle [33], forbidding such a transition; this behavior is reproduced by our calculations. Unfortunately, for finite mass a complete evaluation of $\mathrm{Im}[\Sigma_2(\nu = 0)]$ is out of reach. A simple estimate can be obtained from a golden-rule-type expansion of Σ_2 in T matrices [37], similar to Ref. [57]; we find, in 2D, $\Gamma_2 \sim \gamma^2\beta\frac{\mu^4}{E_b^3}$; in 3D, Γ_2 should still be small in μ/E_b, but the scaling could be different. Putting everything together, an approximate expression for the repulsive polaron spectrum reads

$$\mathcal{A}_2(\nu_2) \simeq (\beta)^{\gamma^2} \frac{\Gamma_2}{\nu_2^2 + \left(\frac{1}{2}\Gamma_2\right)^2} + f_2(\nu_2), \tag{8}$$

where $f_2(\nu_2)$ interpolates between the limits $f_2(\nu_2) \simeq \gamma^2/\sqrt{\beta\mu\nu_2}$ in 2D and $f_2(\nu_2) \simeq \gamma^2/(\beta\mu)$ in 3D, for $\nu_2 \ll \beta\mu$, and $f_2 \simeq 1/\mu(\nu_2/\mu)^{\gamma^2-1}$ for $\nu_2 \gtrsim \beta\mu$. A sketch is shown in Fig. 2 (yellow feature in the lower panel).

Discussion. So far, we have only discussed the spectrum in the molecular limit $E_b \gg \mu$. In the opposite limit, the influence of the bound state should be negligible. The spectrum of a heavy impurity without a bound state was computed in Ref. [51], and we expect the same result here: a single feature of a form similar to the repulsive polaron described above, but with a delta peak that is not broadened, and singularity exponents controlled by $\delta \ll 1$ for $\mu \gg E_b$. Both known limits (in 2D) are sketched in Fig. 4, along with the thresholds as determined from Fumi's theorem, which should be approximately correct for large masses. Note that if we follow the lower spectral feature, we see a "molecule-to-polaron transition," since, for $\mu \ll E_b$, the single-particle spectrum is fully incoherent, but fully coherent in the opposite limit. The details of this transition/crossover [58] remain to be explored. In particular, it would be interesting to analyze this in 3D, where a vacuum bound state only forms at $a > 0$.

Let us also comment on the connection to quantum Monte Carlo and experiments. A major difference is that the Monte Carlo works extract the molecule solely from a pole in the two-particle propagator. The latter was obtained in our recent work [34], and we found essentially opposite behavior to the one presented here, e.g., for $E_b \gg \mu$, there is a sharp feature related to the molecule, and a broad continuum at larger energies. However, here we have argued that the molecule emerges as an incoherent ground-state feature in the single-particle propagator as well. This seems to be in agreement with the ultracold gas experiments in both 3D [1,2,4,5] and 2D [3], while the results of the 2D TMD experiment are somewhat less clear [8]. The incoherent molecule feature was not seen in the "polaron spectra" of the recent Monte Carlo work [22], possibly due to problems with analytical continuation. Finally, let us note that most Monte Carlo works, in 3D [16–18,21,22] and 2D [19,20], deal with the (almost) equal mass case, while in the experiment also heavily mass-imbalanced ^{6}Li-^{40}K mixtures are used. Anyway, we do not expect significant changes in the spectra for equal masses, except for the disappearance of the orthogonality power laws beyond E_{recoil}.

Conclusion. We presented a controlled computation of polaron spectra, providing the connection to the infinite mass limit. We found that, for large binding, the attractive polaron and molecule-hole continuum merge into a single incoherent feature, and also gave a detailed description of the repulsive polaron spectrum. Our work paves the way towards the study of many impurity physics, including the effective interaction between impurities, molecular condensate versus polaron Fermi gas, etc. [59,60].

Acknowledgments. The authors acknowledge very helpful discussions with J. von Delft, L. I. Glazman, O. Goulko, S. Huber, A. Imamoğlu, L. Pollet, N. Prokof'ev, M. Punk, and R. Schmidt. D.P. and M.G. were supported by the German-Israeli Foundation (Grant No. I-1259-303.10). In addition, D.P. was supported by the German Excellence Initiative via the Nanosystems Initiative Munich (NIM), and M.G. was supported by the Israel Science Foundation (Grant No. 227/15), the U.S.-Israel Binational Science Foundation (Grant No. 2014262), and the Israel Ministry of Science and Technology (Contract No. 3-12419).

[1] A. Schirotzek, C.-H. Wu, A. Sommer, and M. W. Zwierlein, Phys. Rev. Lett. **102**, 230402 (2009).

[2] C. Kohstall, M. Zaccanti, M. Jag, A. Trenkwalder, P. Massignan, G. M. Bruun, F. Schreck, and R. Grimm, Nature (London) **485**, 615 (2012).

[3] M. Koschorreck, D. Pertot, E. Vogt, B. Fröhlich, M. Feld, and M. Köhl, Nature (London) **485**, 619 (2012).

[4] M. Cetina, M. Jag, R. S. Lous, I. Fritsche, J. T. Walraven, R. Grimm, J. Levinsen, M. M. Parish, R. Schmidt, M. Knap *et al.*, Science **354**, 96 (2016).

[5] F. Scazza, G. Valtolina, P. Massignan, A. Recati, A. Amico, A. Burchianti, C. Fort, M. Inguscio, M. Zaccanti, and G. Roati, Phys. Rev. Lett. **118**, 083602 (2017).

[6] W. Ketterle and M. W. Zwierlein, in *Ultracold Fermi Gases*, Proceedings of the International School of Physics "Enrico Fermi," Course CLXIV, Varenna, 2006, edited by M. Inguscio, W. Ketterle, and C. Salomon (IOS Press, Amsterdam, 2008).

[7] S. Smolka, W.Wuester, F. Haupt, S. Faelt, W. Wegschneider, and A. Imamoglu, Science **346**, 332 (2014).

[8] M. Sidler, P. Back, O. Cotlet, A. Srivastava, T. Fink, M. Kroner, E. Demler, and A. Imamoglu, Nat. Phys. **13**, 255 (2017).

[9] F. Chevy, Phys. Rev. A **74**, 063628 (2006).

[10] M. Punk, P. T. Dumitrescu, and W. Zwerger, Phys. Rev. A **80**, 053605 (2009).

[11] C. Mora and F. Chevy, Phys. Rev. A **80**, 033607 (2009).

[12] R. Combescot, S. Giraud, and X. Leyronas, Europhys. Lett. **88**, 60007 (2010).

[13] M. M. Parish, Phys. Rev. A **83**, 051603 (2011).

[14] M. M. Parish and J. Levinsen, Phys. Rev. A **87**, 033616 (2013).

[15] J. Levinsen and M. M. Parish, Annu. Rev. Cold At. Mol. **3**, 1 (2015).

[16] N. V. Prokof'ev and B. V. Svistunov, Phys. Rev. B **77**, 020408 (2008).

[17] N. V. Prokof'ev and B. V. Svistunov, Phys. Rev. B **77**, 125101 (2008).

[18] J. Vlietinck, J. Ryckebusch, and K. Van Houcke, Phys. Rev. B **87**, 115133 (2013).

[19] J. Vlietinck, J. Ryckebusch, and K. Van Houcke, Phys. Rev. B **89**, 085119 (2014).

[20] P. Kroiss and L. Pollet, Phys. Rev. B **90**, 104510 (2014).

[21] P. Kroiss and L. Pollet, Phys. Rev. B **91**, 144507 (2015).

[22] O. Goulko, A. S. Mishchenko, N. Prokof'ev, and B. Svistunov, Phys. Rev. A **94**, 051605 (2016).

[23] R. Combescot, A. Recati, C. Lobo, and F. Chevy, Phys. Rev. Lett. **98**, 180402 (2007).

[24] M. Punk and W. Zwerger, Phys. Rev. Lett. **99**, 170404 (2007).

[25] R. Schmidt, T. Enss, V. Pietilä, and E. Demler, Phys. Rev. A **85**, 021602 (2012).

[26] D. K. Efimkin and A. H. MacDonald, Phys. Rev. B **95**, 035417 (2017).

[27] R. Schmidt and T. Enss, Phys. Rev. A **83**, 063620 (2011).

[28] F. B. Kugler and J. von Delft, J. Phys.: Condens. Matter **30**, 195501 (2018).

[29] P. Anderson, Phys. Rev. Lett. **18**, 1049 (1967).

[30] M. Combescot and P. Nozières, J. Phys. **32**, 913 (1971).

[31] M. Baeten and M. Wouters, Phys. Rev. B **91**, 115313 (2015).

[32] R. Schmidt, M. Knap, D. A. Ivanov, J.-S. You, M. Cetina, and E. Demler, Rep. Prog. Phys. **81**, 024401 (2018).

[33] P. Nozières and C. T. De Dominicis, Phys. Rev. **178**, 1097 (1969).

[34] D. Pimenov, J. von Delft, L. Glazman, and M. Goldstein, Phys. Rev. B **96**, 155310 (2017); D. Pimenov, Fermi-edge polaritons with finite hole-mass, Master's thesis, Ludwig Maximilians University of Munich, 2015.

[35] For an exciton to bind two same-spin electrons, the "trion" angular momentum must be odd by Pauli exclusion, and this is energetically unfavorable for heavy excitons [14,61].

[36] This also applies to electronic systems due to screening [34] .

[37] See Supplemental Material at http://link.aps.org/supplemental/10.1103/PhysRevB.98.220302 which includes Refs. [62–64], for further technical details.

[38] We neglect band bottom features discussed in Ref. [32] .

[39] G. Mahan, *Many-Particle Physics*, 3rd ed. (Kluwer Academic/Plenum, New York/London, 2000).

[40] S. K. Adhikari, Am. J. Phys. **54**, 362 (1986).

[41] M. Randeria, J.-M. Duan, and L.-Y. Shieh, Phys. Rev. B **41**, 327 (1990).

[42] P. Bloom, Phys. Rev. B **12**, 125 (1975).

[43] R. Combescot and S. Giraud, Phys. Rev. Lett. **101**, 050404 (2008).

[44] The computation is restricted to a parametrically large window of not too small frequencies, $\mu^2/E_\mathrm{b} \ll \omega + E_\mathrm{b} \ll \mu$ [37] .

[45] G. D. Mahan, Phys. Rev. **153**, 882 (1967).

[46] B. Roulet, J. Gavoret, and P. Nozieres, Phys. Rev. **178**, 1072 (1969).

[47] P. Nozieres, J. Gavoret, and B. Roulet, Phys. Rev. **178**, 1084 (1969).

[48] J. Gavoret, P. Nozieres, B. Roulet, and M. Combescot, J. Phys. (Paris) **30**, 987 (1969).

[49] A. E. Ruckenstein and S. Schmitt-Rink, Phys. Rev. B **35**, 7551 (1987).

[50] P. Nozières, J. Phys. I France **4**, 1275 (1994).

[51] A. Rosch and T. Kopp, Phys. Rev. Lett. **75**, 1988 (1995).

[52] A. Rosch, Adv. Phys. **48**, 295 (1999).

[53] The coefficient in front of β cannot be determined exactly with logarithmic accuracy, but is between γ^2 and 1 [34,48].

[54] X. Cui and H. Zhai, Phys. Rev. A **81**, 041602 (2010).

[55] P. Massignan and G. Bruun, Eur. Phys. J. D **65**, 83 (2011).

[56] V. Ngampruetikorn, J. Levinsen, and M. M. Parish, Europhys. Lett. **98**, 30005 (2012).

[57] G. M. Bruun and P. Massignan, Phys. Rev. Lett. **105**, 020403 (2010).

[58] D. Edwards, J. Phys.: Condens. Matter **25**, 425602 (2013).

[59] L. Radzihovsky and D. E. Sheehy, Rep. Prog. Phys. **73**, 076501 (2010).

[60] H. Hu, B. C. Mulkerin, J. Wang, and X.-J. Liu, Phys. Rev. A **98**, 013626 (2018).

[61] C. J. M. Mathy, M. M. Parish, and D. A. Huse, Phys. Rev. Lett. **106**, 166404 (2011).

[62] I. S. Gradshteyn and I. M. Ryzhik, *Table of Integrals, Series, and Products* (Academic, New York, 2014).

[63] M. Punk, Many-particle physics with ultracold gases, Ph.D. thesis, Technical University of Munich, 2010.

[64] T. Kopp, A. E. Ruckenstein, and S. Schmitt-Rink, Phys. Rev. B **42**, 6850 (1990).